Carbohydrate Polymers 87 (2012) 1073–1080

Contents lists available at SciVerse ScienceDirect

Carbohydrate Polymers

journal homepage: www.elsevier.com/locate/carbpol

Poly(3-hydroxubutyrate-co-4-hydroxubutyrate)/bacterial cellulose composite porous scaffold: Preparation, characterization and biocompatibility evaluation

Cai Zhijiang[a,b,*], Hou Chengwei[a], Yang Guang[a]

[a] School of Textiles, Tianjin Polytechnic University, Tianjin 300160, China
[b] Key Laboratory of Advanced Textile Composites, Ministry of Education of China, Tianjin 300160, China

ARTICLE INFO

Article history:
Received 15 April 2011
Received in revised form 5 July 2011
Accepted 16 August 2011
Available online 22 August 2011

Keywords:
Poly(3-hydroxubutyrate-co-4-hydroxubutyrate)
Bacterial cellulose
Composite scaffold

ABSTRACT

Bio-composite scaffolds were prepared by freeze-drying using poly(3-hydroxubutyrate-co-4-hydroxubutyrate) (P(3HB-co-4HB)) and bacterial cellulose (BC) as raw materials and trifluoroacetic acid (TFA) as co-solvent. The characteristics of the composite scaffold were investigated by field emission scanning electron microscopy (FESEM), Fourier transform infrared spectra (FT-IR), X-ray diffraction (XRD), water contact angle measurement and tensile testing. Preliminary biodegradation test was performed for P(3HB-co-4HB) and P(3HB-co-4HB)/BC composite scaffold in buffer solution and enzyme solution. The biocompatibility of the composite scaffold was preliminarily evaluated by cell adhesion studies using Chinese Hamster Lung (CHL) fibroblast cells. The cells incubated with composite scaffold for 48 h were capable of forming cell adhesion and proliferation, which showed better biocompatibility than pure P(3HB-co-4HB) scaffold. Thus, the prepared P(3HB-co-4HB)/BC composite scaffold was bioactive and may be suitable for cell adhesion/attachment suggesting that these scaffolds can be used for wound dressing or tissue-engineering scaffolds.

1. Introduction

Natural poly(3-hydroxybutyrate) (PHB) is a saturated aliphatic polyester synthesized and accumulated by a variety of bacteria as a reserve energy source (Gloria, Reyes, & So, 1997; Zahra et al., 2009). PHB has many remarkable characteristics such as biodegradability, biocompatibility, optical activity and blood clotting (Savenkova et al., 2000; Zhao, Deng, Chen, & Chen, 2003). It is a truly biodegradable material suitable for two promising applications: one is as a viable candidate for relieving environmental concerns caused by disposal of non-degradable plastic; the other is to provide a new-type biomedical materials. PHB has also been evaluated for a variety of medical applications, which include controlled release systems (Colin & Saghir, 1996), surgical sutures (Baspist & Ziegler, 1982), wound dressing (Hu, Jou, & Yang, 2003), orthopedic uses (Wang, Wu, & Chen, 2004) and as a pericardial substitute. In recent years, PHB has been studied as biopolymer porous substrates in tissue engineering applications (Boeree, Dove, Cooper, Knowles, & Hastings, 1993; Doyle, Tanner, & Bonfield, 1991), especially for tissue engineering scaffold with high mechanical properties (Korakot, Neeracha, Prasit, & Pitt, 2007; Liudmila, Jonas, Maria, Mikael, & Lev, 2008; Zhou et al., 2010). The PHB biopolymer provides a means to target a wide range of tissues with potential product applications for the cardiovascular system, cornea, pancreas, gastrointestinal system, kidney and genitourinary system, musculoskeletal system, nervous system, teeth and oral cavity, skin and so forth (Ji, Li, & Chen, 2008; Qu, Wu, Liang, Zou, & Chen, 2006; Thomson et al., 1996). However, its utilization has been limited due to its inherent physical and chemical properties such as brittleness and hydrophobicity (Koning & Lemstra, 1993). In order to improve these properties, various methods, especially blending with another kind of polymer, has been investigated. PHB has been reported to be miscible with a few chemically synthesized polymers, such as poly(ethylene oxide) (Chee, Ismail, Kummerlöwe, & Kammer, 2002), poly(vinylidene fluoride) (Akira, 2006) and highly saponified poly(vinyl alcohol) (Tetsuya, Naoko, & Yoshio, 1999; Yuki et al., 2007). Biosynthesis of co-polyester containing 3-hydroxyalkanoates (3HA) units, such as poly(3-hydroxubutyrate-co-3-hydroxyvalerate) (Andrij, Nadine, Cathrin, & Adler, 2006) has also been extensively studied. Preliminary studies which used PHB chain segments obtained by the degradation of natural-origin PHB for the synthesis of PHB-containing block copolymers have been reported (Gamal & Hartmut, 2004; Li et al., 2006). Yalpani, Marchessault, Moin, & Monaseterios (1991) have demonstrated the use of degraded natural-origin PHB for the synthesis of PHB-polysaccharide conjugates.

Bacterial cellulose (BC) is another kind of natural polymer produced by strains of the bacterium *Acetobacter xylinum*, which is a

* Corresponding author at: School of Textiles, Tianjin Polytechnic University, No 63 ChenLin Street, HeDong District, Postcode 300160, Tianjin, China.
Tel.: +86 22 24538385; fax: +86 22 24528187.
E-mail address: caizhijiang@hotmail.com (C. Zhijiang).

0144-8617/$ – see front matter © 2011 Elsevier Ltd. All rights reserved.
doi:10.1016/j.carbpol.2011.08.037

Gram-negative, rod shaped and strictly aerobic bacterium. It has very high purity and contains no lignin, hemicelluloses, pectin, and waxes as plant cellulose does. BC differs from plant cellulose with respect to its high crystallinity, ultra-fine network structure, high hydrophilicity, high mechanical properties and biocompatibility (Eichhorn et al., 2001; Klemm, Schumann, Udhardt, & Marsch, 2001). BC has long been used in a variety of applications such as diaphragms in speakers and headphones (Iguchi, Yamanaka, & Budhiono, 2000), paper making (Hioki et al., 1995), separation membranes (Takai, 1994), and electro-conductive carbon film (Yoshino et al., 1991). Owing to its biocompatibility, BC has also recently attracted a great deal of attention for biomedical applications. For instance, BC has been successfully used as artificial skin for burn or wound healing material (Alvarez, Patel, Booker, & Markowitz, 2004; Czaja, Krystynowicz, Bielecki, & Brown, 2006; Legeza et al., 2004), artificial blood vessels for microsurgery (Klemm et al., 2001). The potential of BC scaffold for in vitro and in vivo tissue regeneration also continues to be explored and shows great promise (Backdahl et al., 2006; Helenius et al., 2006).

For tissue engineering, fundamental knowledge of cell-substrate interactions is very important. Topographical cues, independent of biochemistry, generated by an extracellular matrix (ECM) may have significant effects on cellular behavior (Flemming, Murphy, Abrams, Goodman, & Nealey, 1999; Wojciak-Stothard, Curtis, Monaghan, Macdonald, & Wilkision, 1996). In general, the tissue development is controlled in three matrix size scales. The gross shape and size of tissue is decided by the macroscopic shape (cm to mm scale) of matrix; cell invasion and growth is controlled by the size and structure of the matrix pore (μm). The adhesion and gene expression of cells are adjusted by the surface chemistry of the matrices (nm scale).

In our previous work (Cai, Yang, & Kim, 2011), we use wet pellicle BC to prepare PHB/BC nanocomposite. In this study, we use poly(3-hydroxubutyrate-co-4-hydroxubutyrate) (P(3HB-co-4HB)) as raw material. We are interested in the preparation and characterization of P(3HB-co-4HB)/BC bio-composite porous scaffold by freeze-drying method using trifluoroacetic acid (TFA) as co-solvent. Bio-composite scaffold were characterized by field emission scanning electron microscopy (FESEM), Fourier transform infrared spectra (FT-IR) and X-ray diffraction (XRD). The mechanical properties, biodegradability and biocompatibility of the P(3HB-co-4HB)/BC bio-composite scaffold were also evaluated.

2. Materials and methods

2.1. Materials

The poly(3-hydroxubutyrate-co-4-hydroxubutyrate), a white powder sample was kindly provided by Tianjin GuoYun Biomaterial Co. Ltd. (Tianjin, China), $M\eta = 3.7 \times 10^5$ (obtained by G.P.C. in chloroform at 30 °C). Chloroform and other chemicals of the highest purity available were used and were purchased from Sigma–Aldrich. Trifluoroacetic acid (>99%) was purchased from Daejung Chemical & Metals Co. Ltd.

2.2. Preparation of bacterial cellulose pellicles

The bacterium, *Gluconacetobacter xylinum JC-6*, was cultured on Hestrin and Schramm (HS) medium, which was composed of 2% (w/v) glucose, 0.5% (w/v) yeast extract, 0.5% (w/v) bacto-peptone, 0.27% (w/v) disodium phosphate, and 0.115% (w/v) citric acid. All the cells were pre-cultured in a test tube. After a small cellulose pellicle formation on the surface of the medium, it was removed and inoculated into a 500 mL Erlenmeyer flask containing 100 mL of the HS medium. The flasks were incubated statically at 30 °C for 14 days. The cellulose pellicles were dipped into 0.25 M NaOH for 48 h at room temperature in order to eliminate the cells and components of the culture liquid. The pH was then lowered to 7.0 by repeated washing with distilled water. The purified cellulose pellicles were freeze-dried

2.3. Preparation of PHB/BC composite porous scaffolds

Dried bacterial cellulose pellicles were cut into small pieces. Then bacterial cellulose was mixed with P(3HB-co-4HB) powder at weight ratio 50:50 and dissolved in trifluoroacetic acid at room condition to make a 2 wt% solution. The transparent P(3HB-co-4HB)/bacterial cellulose blend solution was kept in sealed glass bottle. P(3HB-co-4HB)/BC composite porous scaffold was prepared by drying the solution using freeze-dryer (IP3 Jouan, France) at −40 °C for 6 days to remove the TFA completely.

2.4. Porosity measurements

The porosity of scaffold was estimated using Archimedes' principle based on fluid displacement measurement techniques (Lee et al., 2003). Briefly, the initial and final volume of water in a graduated cylinder before and after scaffold (disc-shaped: 10 mm diameter, 5 mm thickness) immersion was recorded. After 1 h, scaffolds were removed from the cylinders and the volume of the remaining water was also recorded. The degree of porosity was then determined by calculating the volume of free space within the material with respect to the total volume of the scaffold ($n = 5$). Since scaffold porosity was measured in an aqueous solution, it was important to correct for the effect of polymer swelling on porosity. Thus, the degree of swelling for pure bacterial cellulose and PHB scaffolds (equivalent volume to porous scaffolds) following 1 h of immersion in water at room temperature were determined.

2.5. Characterization

For characterization, the samples of P(3HB-co-4HB), BC and P(3HB-co-4HB)/BC composite scaffold were prepared by freeze-drying under the same conditions. For field emission scanning electron microscopy observations, samples of P(3HB-co-4HB), BC and P(3HB-co-4HB)/BC composite scaffold were sputter coated with gold. The morphology of surface and cross-section was observed with a Hitachi S-4300 scanning electron microscopy at an accelerating voltage of 15 kV. Fourier transform infrared spectra were obtained using a Perkin-Elmer System 2000 FT-IR spectrophotometer. X-ray diffraction patterns were recorded on an X-ray diffractometer (D/MAX-2500, Rigaku), by using Cu K(radiation at 40 kV and 30 mA. The diffraction angle ranged from 5° to 40°. Tensile test specimens were prepared by cutting the membranes to 10 mm wide and 65 mm long strips using a precision cutter. Young's modulus of samples were found from the tensile test results conducted according to ASTM D-882-97 as a standard test method for tensile elastic properties of thin plastic sheeting. Tensile test was done on a universal testing machine in ambient condition. Two ends of the specimens were placed between the upper and lower jaws of the instrument, leaving a length of 50 mm of the film in between the two jaws. Extension speed of the instrument was 2 mm/min. Water contact angle measurement was performed at 25 °C in the range of 0.5–20 min by pendant drop method, employing a contact-angle measurement apparatus (type DSA-10, made in KURSS Company, Germany). For each sample, the mean of five separate points was obtained based on the same contact time.

2.6. Evaluation of biodegradability

The biodegradation studies of the P(3HB-co-4HB) and P(3HB-co-4HB)/BC composite scaffold were conducted at 37 °C in buffer solutions (pH 7.0) and in 0.1 M phosphate buffer(PBS, Oxoid pH: 7.2–7.4) containing lysozyme (Sigma, 0.2% solution in PBS). The dried scaffolds were cut into squares and incubated in the reaction solution with shaking, and at various time points the samples were removed, washed in distilled water and allowed to dry in air to constant weight. For each test, three samples were used and the degradation rate (S%) was determined by the ratio of the weight loss to the initial weight of samples as shown below.

$$S = \frac{W_0 - W_t}{W_0} \times 100\% \quad (1)$$

where S is the degradation rate, W_t and W_0 are the weight of samples after dried and the initial weight respectively.

2.7. Evaluation of cell biocompatibility

2.7.1. Preparation of samples

The P(3HB-co-4HB) and P(3HB-co-4HB)/BC composite cylinder scaffolds (20 mm diameter × 4 mm height) were prepared and sterilized by gamma irradiation. Chinese Hamster Lung cells (CHL) were used in the study and were cultured in Dulbecco's Modified Eagles Medium (DEME/F-12), supplemented with gentamicin (50 μg/mL), 10% fetal calf serum (FCS) and 5.6% sodium bicarbonate adjusted to pH 7.0–7.4.

2.7.2. Cell culture

The prepared samples were placed in the bottom of each well of a 24-well tissue-culture plate. Single-cell suspensions were added to the samples at a density of 1.5×10^4 cells/mL. And the samples were incubated in 1 mL medium for 48 h at 37 °C/5% CO_2.

2.7.3. Determination of cell adhesion and growth

For the measurement of cell adhesion, cells were washed twice with PBS to remove non-adherent cells and the attached cells were fixed with 2.5% glutaraldehyde buffer solution (pH 7.4) at 4 °C for 12 h. Furthermore, the samples were rinsed in distilled water and dehydrated by immersing them in increasing concentrations of ethanol (10%, 30%, 50%, 60%, 70%, 80%, 90%, 95% and 100%) for about 20 min at each concentration. For each experimental value, three independent experiments were conducted. The cells' morphology on samples surface was observed by FESEM, and the cells number, at eight random fields, were counted visually.

3. Results and discussion

3.1. FESEM observation

As seen from Fig. 1a, porous structure can be observed on the surface of pure P(3HB-co-4HB) scaffold prepared by freeze-drying method. The mean diameter of these porous is about 50 μm. From the cross sectional image (Fig. 1b), we also can see porous structure with about 50 μm in diameter. The porosity of the pure P(3HB-co-4HB) scaffold is about 92%, which indicates that the scaffold has good pores interconnection. However, none of nano-scaled microspores with diameter less than 1 μm can be detected. For BC, it has quite different structure from that of P(3HB-co-4HB) due to different synthesis procedure. During cultivation, the bacteria synthesize fine sub-elementary cellulose fibrils, which are extruded from terminal enzyme complexes into the culture medium. Nascent cellulose extending from terminal enzyme complexes is initially amorphous and is gradually crystallized to cellulose I. The sub-elementary fibrils are approximately 2–4 nm in diameter and are assembled into microfibrils. These microfibrils are then bundled to form ribbon-shaped fibrils of approximately 4 (thickness) × 80 (width) nm. Fig. 1c and d present typical FESEM images of freeze-dried BC. As seen from Fig. 1c, BC ribbon-shaped fibrils can be observed on the surface. The mean diameter of these fibrils is about 100 nm. From cross sectional images (Fig. 1d) we can see that these fibrils assemble together forming porous structure with high aspect ratio. Evidently, a well-organized three-dimensional (3D) network structure is observed. The porosity of the pure BC scaffold is about 85%.

For P(3HB-co-4HB)/BC composite scaffold, it is very interesting to see that the scaffold had multi-pore size distribution. Medium pores with about 20 μm in diameter are uniformly dispersed on the surface (Fig. 1e), which has been observed in the porous polylactic (PLA) system made by freeze-drying (Chen, Ushida, & Tateishi, 2000). More interestingly we find micro-pores with about 500 nm in diameter inside (Fig. 1f) the wall. The medium pores are attributed to the existence of P(3HB-co-4HB), while the micro-pores structure is formed by nanofibrils assembling together during the regeneration process. In the results, a P(3HB-co-4HB)/BC composite scaffold with three-dimensional network structure composing of multi-distribution of pore size is constructed. The porosity of the P(3HB-co-4HB)/BC composite scaffold is about 91%, which is very close to that of pure P(3HB-co-4HB) scaffold. This multi-distribution of pore size structure with high porosity may favor transferring nutrient fluid and waste effectively so as to benefit cell growth in the scaffold.

3.2. FT-IR spectroscopy

FT-IR spectra obtained from pure P(3HB-co-4HB), BC and P(3HB-co-4HB)/BC composite scaffold are shown in Fig. 2. For pure P(3HB-co-4HB) (Fig. 2a), the peak at 3433 cm^{-1} refers to hydroxyl end groups. Peaks at 2973 cm^{-1}, 2889 cm^{-1} and 2741 cm^{-1} refer to C–H stretching vibration. A sharp and steep band observed at 1726 cm^{-1} is assigned to C=O stretching vibration. The peak at 1283 cm^{-1} refers to C–O stretching vibrations. For pure BC (Fig. 2b), a broad band at 3300 cm^{-1} is attributed to O–H stretching vibration. Band at 2820 cm^{-1} represents the aliphatic C–H stretching vibration. Absorbance peak at wave number 1730 cm^{-1} is attributed to hydrogen-bonded carbonyl stretching vibration. Absorbance peak at wave number 1427 cm^{-1} is assigned to CH_2 symmetric bending vibration. A sharp and steep band observed at 1080 cm^{-1} is due to the presence of C–O–C stretching vibrations. The peak at 684 cm^{-1} is assigned to OH out-of-phase bending vibrations. Spectra obtained for P(3HB-co-4HB)/BC composite scaffold (Fig. 2c) display basically the bands observed for the two individual components.

3.3. XRD analysis

Yokouchi, Chatani, Tadokoro, Teranishi, & Tani (1973) had reported that PHB crystallizes in an orthorhombic lattice structure ($P2_12_12_1$: a = 0.576 nm, b = 1.320 nm and c = 0.596 nm (fiber axis), α-form) with their chains in the left 2/1 helix. For P(3HB-co-4HB) (Fig. 3a), the characteristic XRD diffractogram is same to PHB only the scattering intensity decreases, which means the crystallinity and regularity become less due to the copolymerization. Two strong scattering intensity peaks are detected at 2θ value of 13° and 17° assigned to be (0 2 0) and (1 1 0) of the orthorhombic unit cell, respectively. Regarding the crystalline structure of cellulose fibers, it is known to be classified into four crystallization types, viz. cellulose I, II, III and IV, and their crystalline structure are able to be transformed form one type to another (Jung, Benerito, Berni, & Mitcham, 1977). For bacterial cellulose, two main scattering intensity peaks can be identified at 2θ value of 14.2° and 22.4° as shown in

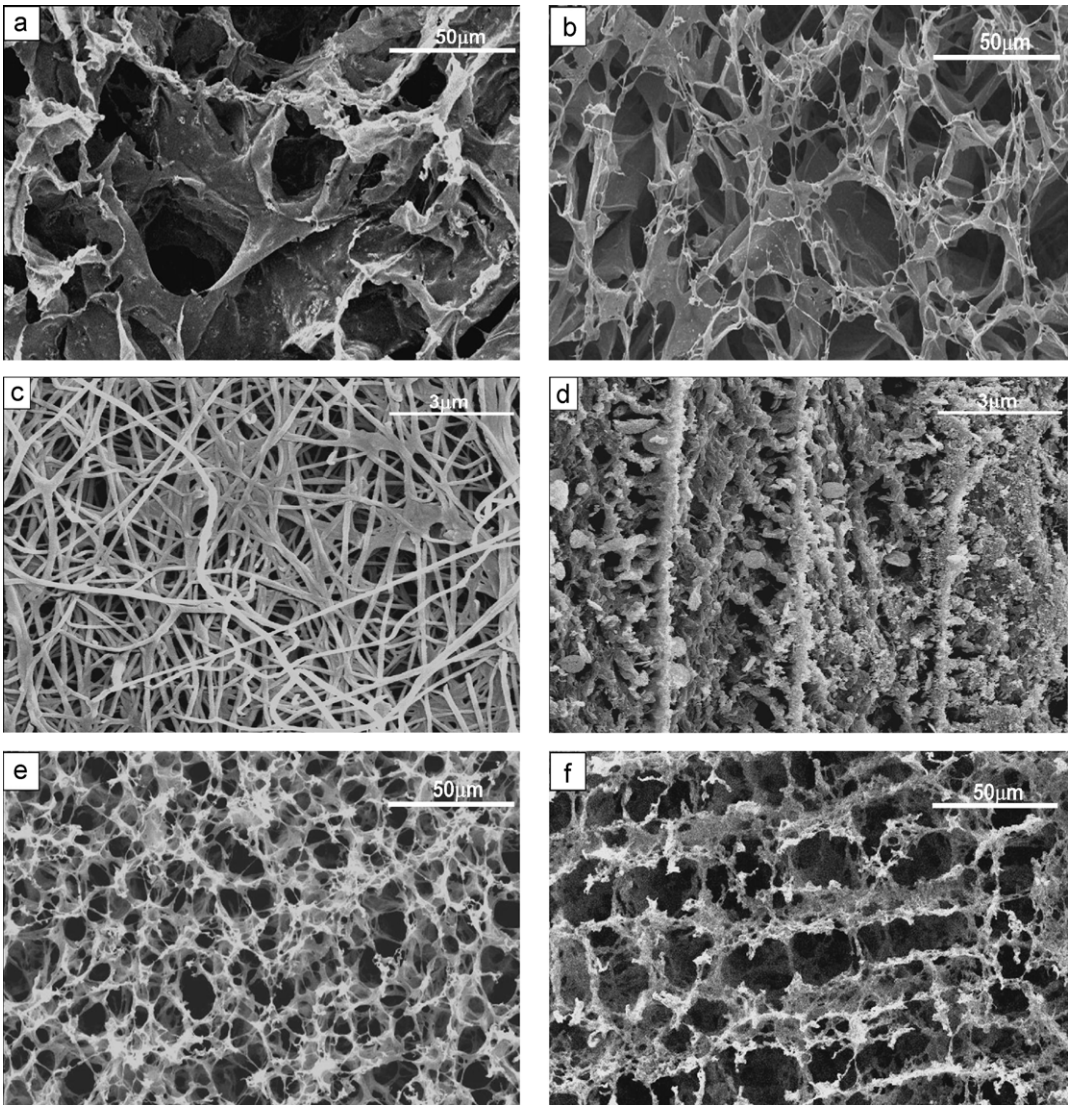

Fig. 1. FESEM images of P(3HB-co-4HB) (a: surface morphology; b: cross-section morphology), BC (c: surface morphology; d: cross-section morphology) and P(3HB-co-4HB)/BC nanocomposite scaffolds (e: surface morphology; f: cross-section morphology).

Fig. 3c, which are assigned to the (1 $\bar{1}$ 0) and (2 0 0) reflexions planes of cellulose I (Tokoh, Takabe, Fujita, & Saiki, 1998). For P(3HB-co-4HB)/BC composite scaffold (Fig. 3b), diffraction patterns show the P(3HB-co-4HB) characteristic peaks with a decrease intensity and cellulose II characteristic peaks due to the regeneration of BC. Originally, X-ray diffraction peaks of cellulose II appear at 12.1°, 19.8° and 22° assigned to (1 1 0), (1 $\bar{1}$ 0), and (2 0 0).

3.4. Tensile test

To investigate the mechanical characteristics of PHB/BC composite scaffold, the tensile tests were performed according to ASTM D-882-97 standard test method. Table 1 shows mechanical properties of P(3HB-co-4HB), BC and P(3HB-co-4HB)/BC composite scaffold calculated from the stress-strain curves. For P(3HB-co-4HB), it shows roughness properties. Yielding point can be observed in the stress-strain curve. For BC, it shows brittle properties. No yielding point can be observed and the elongation at break is very small. For P(3HB-co-4HB)/BC composite scaffold, we can see a yielding point although it is very close to the breaking point. The tensile strength is about 24 MPa, 114 MPa and 46 MPa for P(3HB-co-4HB), BC and P(3HB-co-4HB)/BC composite scaffold, respectively. And the elongation at break is about 23.5%, 6.5% and 13.5% for P(3HB-co-4HB), BC and P(3HB-co-4HB)/BC composite scaffold, respectively. The Young's modulus found from the slope of the curve is 0.18 GPa for P(3HB-co-4HB), 2.6 GPa for pure BC and 0.88 GPa for P(3HB-co-4HB)/BC composite scaffold. The P(3HB-co-4HB)/BC composite scaffold displays 90% of improvement in tensile strength, 40% of decrease in elongation at break, and 3800% of increase in Young's modulus compared with pure P(3HB-co-4HB). This behavior can be due to the combination of PHB with bacterial cellulose microfibrils with good interfacial adhesion and the formation of strong interactions between P(3HB-co-4HB) and BC chains.

Table 1
Mechanical properties of P(3HB-co-4HB), BC and P(3HB-co-4HB)/BC composite scaffold.

	Tensile strength (MPa)	Elongation at break (%)	Young's modulus (GPa)
P(3HB-co-4HB)	24.63 ± 3.6	23.56 ± 4.4	0.184 ± 0.054
BC	114.45 ± 10.6	6.56 ± 1.3	2.64 ± 0.41
P(3HB-co-4HB)/BC	46 ± 4.5	13.56 ± 3.2	0.88 ± 0.24

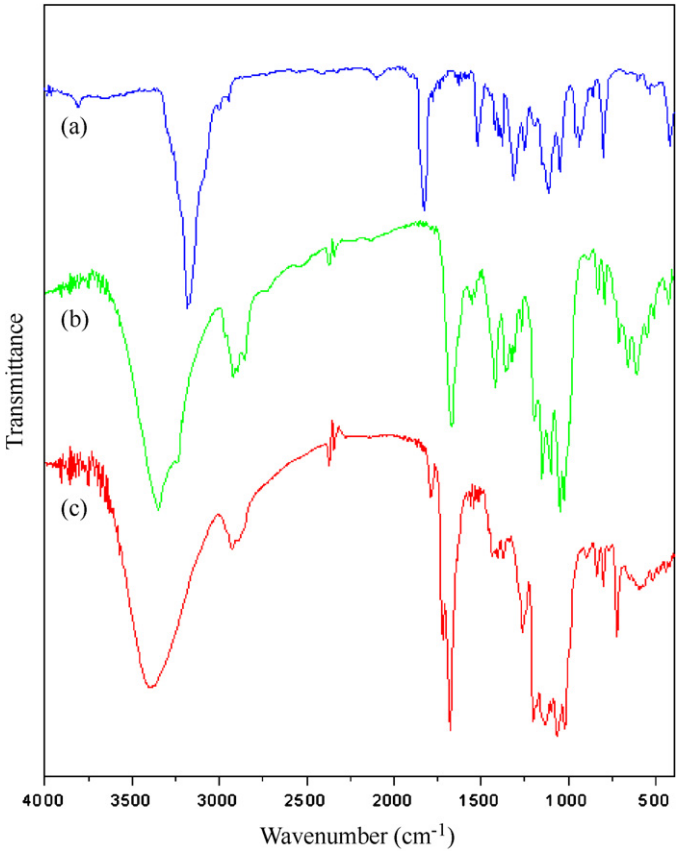

Fig. 2. FT-IR spectra of P(3HB-co-4HB) (a), BC (b) and P(3HB-co-4HB)/BC composite scaffold (c).

At the same time, inherently high modulus and strength of BC allow the mechanical properties of P(3HB-co-4HB)/BC composite scaffold to improve.

3.5. Hydrophilicity

The surface energy of the solid can be estimated by contact angle measurement together with a theory of intermolecular forces. In this experiment, the drop contour analysis was used for determining the surface tension and the water contact angle. The water contact angle and surface tension of the P(3HB-co-4HB), P(3HB-co-4HB)/BC composite scaffold and BC are shown in Fig. 4. For pure BC, the water contact angle value is very small and close to 0°, which

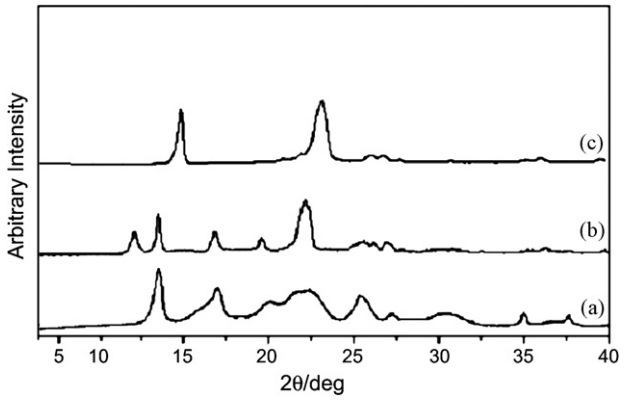

Fig. 3. XRD patterns of P(3HB-co-4HB) (a), P(3HB-co-4HB)/BC composite (b), and BC (c).

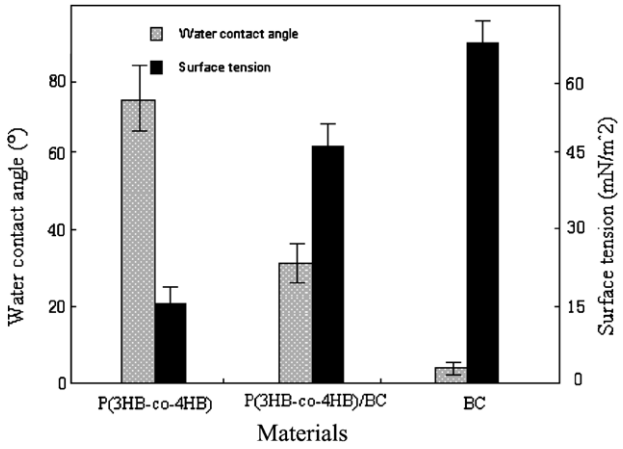

Fig. 4. Water contact angle and surface tension of P(3HB-co-4HB), BC and P(3HB-co-4HB)/BC composite scaffold.

means BC has very high hydrophilicity. However, for pure P(3HB-co-4HB), the water contact angle value is 72.2°. While by blending BC with P(3HB-co-4HB), the water contact angle value reduces to 33.6°. The surface tension value of pure P(3HB-co-4HB) is about 20.5 mN/m^2. With the BC introduction the surface tension value of composite scaffold is up to 59.2 mN/m^2. These results indicate that the hydrophilic property of P(3HB-co-4HB)/BC composite scaffold is much better than pure P(3HB-co-4HB). Such a result is probably accounted for by the high hydrophilicity of BC and the specific interaction involving the carbonyl group of P(3HB-co-4HB) and the –OH in BC. It can be expected that the P(3HB-co-4HB)/BC composite scaffold with high hydrophilicity is more suitable for cell adhesion and proliferation than pure P(3HB-co-4HB).

3.6. Biodegradation tests

It has been reported that PHB can be degraded by many enzymes, for example, depolymerase from *Alcaligenes faecalis T1* (Tanio et al., 1982), *Pseudomonas lemoignei* (Scandola et al., 1997) etc. In vivo, enzymes such as lysozyme may also accelerate the degradation rate of PHB. In this study, degradation rate of P(3HB-co-4HB) and P(3HB-co-4HB)/BC composite scaffold was tested by measuring the weight loss as they were degraded by buffer solution and PBS/lysozyme buffer solution at 37 °C and the results were plotted in Fig. 5. Pure P(3HB-co-4HB) is degraded with a relatively low biodegradation rate in the scale of the experiment. After degradation for 30 days, the weight loss ratio is less than 7% of original weight, which is much faster than that of buffer solution without enzyme. Blending with BC, the degradation rate of P(3HB-co-4HB)/BC composite scaffold was improved. After degradation for 30 days, the weight loss ratio is about 12% of original weight. This acceleration of the biodegradation is supposed to arise from the lowered crystallinity of P(3HB-co-4HB). Another possible reason is the hydrophilicity of the BC, which makes the enzyme easier to attack. Therefore, the acceleration of the biodegradation is caused by a combined effect of lower crystallinity and better hydrophilicity as well.

The variation of pH in buffer solution was accurately measured using pH meter. The initial pH value of buffer solution is 7.0. With degradation time increasing, the pH value of buffer solution tends to decrease. For example, after 20 days' degradation the pH value is 6.4 and after 30 days' degradation the pH value is 6.1. This result might be due to the production of hydroxybutyric acid during the degradation process.

The surface morphology of P(3HB-co-4HB) and P(3HB-co-4HB)/BC composite scaffold degradation in buffer solution and

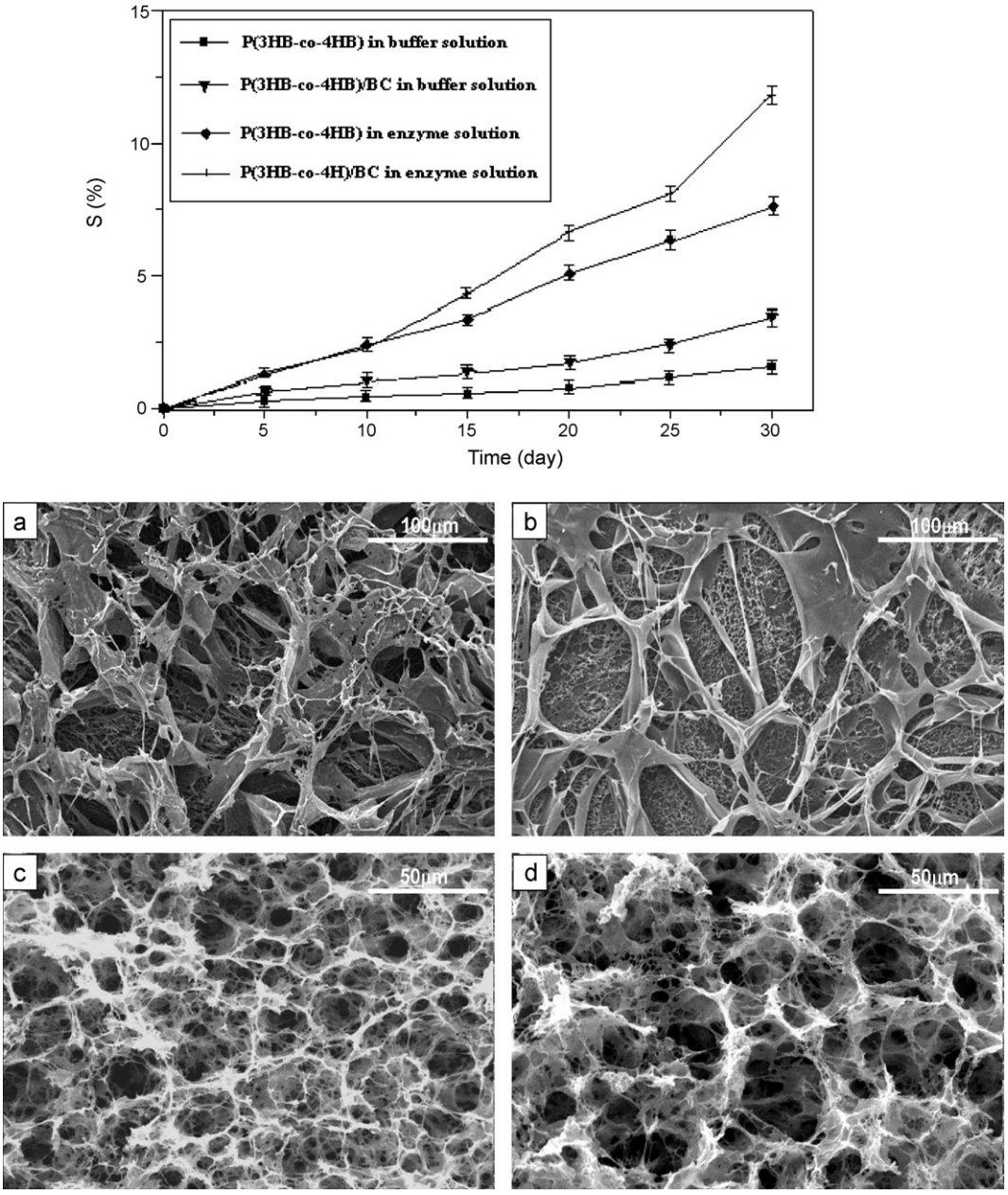

Fig. 5. The degradation rates and surface morphology of P(3HB-co-4HB) (a and b) and P(3HB-co-4HB)/BC (c and d) composite scaffold in buffer solution (a and c) and enzyme solution (b and d).

enzyme solution are shown in Fig. 5. Buffer solutions produce more diffuse surface degradation, whereas degradation in enzyme solutions appears to be more aggressive, with specific sites of attack occurring that produce deep points of surface erosion. The enzymatic biodegradation proceeds from amorphous regions on the surface and erosion develops gradually to the inside. After degradation for 30 days, pore size becomes much bigger and much corrosive behavior can be seen for enzymatic biodegradation since some of the porous network structure collapse.

3.7. Cell compatibility

Cell cytotoxicity testing is one of important factor that affected the use of polymers in tissue engineering. In this study, Chinese Hamster Lung fibroblast was used to evaluate cell compatibility for pure P(3HB-co-4HB), BC and P(3HB-co-4HB)/BC scaffold via cell cultivation in vitro. As shown in Table 2, live cells adhered on the surface of P(3HB-co-4HB)/BC scaffold are much more compared with pure P(3HB-co-4HB) scaffold. In generally, cells do not grow on a solid polymer surface. In fact, cells grow on a layer of protein that interacts with cellular receptors. Blending with BC, P(3HB-co-4HB)/BC composite scaffold becomes more hydrophilic and easy to adsorption proteins.

Table 2
The number of live cells adhered on the surface of materials after incubation for 24 h at 37 °C.

Materials	Number of live cells ($10^8/m^2$)[a]
P(3HB-co-4HB)	14.65 ± 1.46
P(3HB-co-4HB)/BC	21.44 ± 2.11

[a] The number of live cells adhered on the surface of materials was calculated by geometrical average.

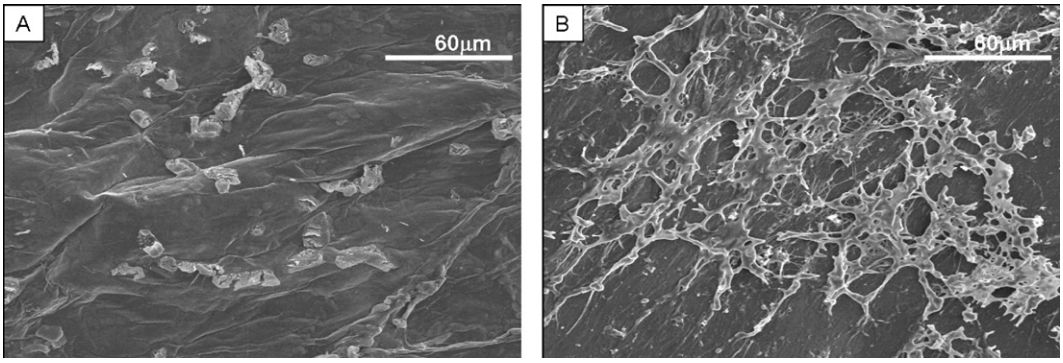

Fig. 6. CHL fibroblast cells attachments of pure P(3HB-co-4HB) (A) and P(3HB-co-4HB)/BC composite scaffold (B) of 48 h seeding the cells.

Fig. 6 shows the morphology of CHL cultured pure P(3HB-co-4HB) and P(3HB-co-4HB)/BC composite scaffold at 37 °C for 48 h. In the case of pure P(3HB-co-4HB), most of the cells are still round-shaped which indicate that the mono-pore P(3HB-co-4HB) scaffold has poor cell adhesion (Fig. 6A). However, in the case of P(3HB-co-4HB)/BC composite scaffold, cells cultured on the scaffold adhere and completely spread on the surface (Fig. 6B). They have many pseudopodia and form a layer on the surface. These results indicate that the cells stretch their morphology and are proliferating. At the same time, live cell adhesion on the surface of multi-pore size scaffold is much more than that of on mono-pore size pure P(3HB-co-4HB) scaffold. Cells cultured on the matrix stretch their morphology maintain their phenotype and the cellular interaction between the cells and the polymer is inseparable. This preliminary experiment suggests that P(3HB-co-4HB)/BC composite scaffold with multi-pore size distribution has better biocompatibility compared with pure P(3HB-co-4HB) scaffold with mono-pore size in terms of fibroblast cell culture. The reason might be due to the appearance of nano scale pores in the multi-pore size scaffold which can adjust the surface chemistry to improve the adhesion of cells. Moreover, the multi-pore size scaffold can offer the diffusion of molecules important to cell survival if the porosity if truly interconnected. It would have potentials to be used as tissue regeneration scaffold in vitro. Further investigation such as cellular proliferation and differentiation assays are underway.

4. Conclusions

In this paper, a novel bio-composite scaffold consisting of P(3HB-co-4HB) and BC, both of which are biocompatible, has been successfully prepared by freeze-drying using TFA as co-solvent. FESEM images show that P(3HB-co-4HB)/BC composite scaffold has three-dimensional network structure composing of multi-distribution pore size. FT-IR and XRD test results confirm the existence of P(3HB-co-4HB) and BC in the composite scaffold. In addition, an great increase in hydrophilicity and mechanical properties is observed for P(3HB-co-4HB)/BC composite scaffold compared with pure P(3HB-co-4HB) scaffold. Preliminary biodegradation test shows that biodegradation rate of P(3HB-co-4HB) can be improved by blending BC. Cell compatibility studies were carried out using CHL fibroblast cells. The cells incubated with P(3HB-co-4HB)/BC composite scaffold for 48 h are capable of forming cell adhesion and proliferation. It shows much better biocompatibility compared with pure P(3HB-co-4HB). So, the prepared P(3HB-co-4HB)/BC composite scaffold is bioactive and may be suitable for cell adhesion/attachment suggesting that these scaffolds can be used for wound dressing or tissue-engineering applications.

Acknowledgement

This work was supported by Tianjin Municipal Natural Science Foundation under the contract of 11JCYBJC02500.

References

Akira, K. (2006). Unique orientation textures formed in miscible blends of poly(vinylidene fluoride) and poly[(*R*)-3-hydroxybutyrate]. *Polymer*, *47*(10), 3548–3556.

Alvarez, O. M., Patel, M., Booker, J., & Markowitz, L. (2004). Effectiveness of biocellulose wound dressing for the treatment of chronic venous leg ulcers: Results of a single center randomized study involving 24 patients. *Wounds*, *16*, 224–233.

Andrij, P., Nadine, S., Cathrin, C., & Adler, H. P. (2006). Preparation of poly(3-hydroxybutyrate-*co*-3-hydroxyvalerate) (PHBV) particles in O/W emulsion. *Polymer*, *47*(6), 1912–1920.

Backdahl, H., Helenius, G., Bodin, A., Nannmark, U., Johansson, B. R., Risberg, B., et al. (2006). Mechanical properties of bacterial cellulose and interactions with smooth muscle cells. *Biomaterials*, *27*(9), 2141–2149.

Baspist J.N. & Ziegler J.B., (1982), *Method of Making Absorbable Surgical Sutures From Poly(Hydroxyacid)*. E.P No. 46334.

Boeree, N. R., Dove, J., Cooper, J. J., Knowles, J., & Hastings, G. W. (1993). Development of a degradable composite for orthopaedic use: Mechanical evaluation of an hydroxyapatite-polyhydroxybutyrate composite material. *Biomaterials*, *14*, 793–796.

Cai, Z., Yang, G., & Kim, J. (2011). Biocompatible nanocomposites prepared by impregnating bacterial cellulose nanofibrils into poly(3-hydroxybutyrate). *Current Applied Physics*, *11*, 247–250.

Chee, M. J. K., Ismail, J., Kummerlöwe, C., & Kammer, H. W. (2002). Study on miscibility of PEO and PCL in blends with PHB by solution viscometry. *Polymer*, *43*(4), 1235–1239.

Chen, G., Ushida, T., & Tateishi, T. (2000). Hybrid biomaterials for tissue engineering: A preparative method for PLA or PLGA-collagen hybrid sponges. *Advanced Materials*, *12*, 455–457.

Colin, W. P., & Saghir, A. (1996). Biosynthetic polyhydroxyalkanoates and their potential in drug delivery. *Advanced Drug Delivery Reviews*, *18*, 133–162.

Czaja, W., Krystynowicz, A., Bielecki, S., & Brown, R. M. (2006). Microbial cellulose – The natural power to heal wounds. *Biomaterials*, *27*(2), 145–151.

Doyle, C., Tanner, E. T., & Bonfield, W. (1991). In vitro and in vivo evaluation of polyhydroxybutyrate and of polyhydroxybutyrate reinforced with hydroxyapatite. *Biomaterials*, *12*, 841–847.

Eichhorn, S. J., Baillie, C. A., Zafeiropoulos, N., Mwaikambo, L. Y., Ansell, M. P., Dufresne, A., et al. (2001). Review current international research into cellulosic fibres and composites. *Journal of Materials Science*, *36*(9), 2107–2131.

Flemming, R. G., Murphy, C. J., Abrams, G. A., Goodman, S. L., & Nealey, P. F. (1999). Effects of synthetic micro-and nano-structured surfaces on cell behavior. *Biomaterials.*, *20*, 573–588.

Gamal, R. S., & Hartmut, S. (2004). Biodegradable copolymers based on bacterial Poly((R)-3-hydroxybutyrate): Thermal and mechanical properties and biodegradation behavior. *Polymer Degradation and Stability*, *83*(1), 101–110.

Gloria, D., Reyes, R. S., & So, M. M. U. (1997). Isolation, screening and identification of bacteria for poly-β-hydroxybutyrate (PHB) production. *Studies in Environmental Science*, *66*, 737–748.

Helenius, G., Backdahl, H., Bodin, A., Nannmark, U., Gatenholm, P., & Risberg, B. (2006). In vivo biocompatibility of bacterial cellulose. *Journal of Biomedical Materials Research Part A*, *76*(2), 431–438.

Hioki, N., Hori, Y., Watanabe, K., Morinaga, Y., Yoshinaga, F., Hibino, Y., et al. (1995). Bacterial cellulose as a new material for papermaking. *Japan TAPPI Journal*, *49*, 718–723.

Hu, S. G., Jou, C. H., & Yang, M. C. (2003). Antibacterial and biodegradable properties of polyhydroxyalkanoates grafted with chitosan and chitooligosaccharides via ozone treatment. *Journal of Applied Polymer Science*, *88*, 2797–2803.

Iguchi, M., Yamanaka, S., & Budhiono, A. (2000). Bacterial cellulose – A masterpiece of nature's arts. *Journal of Materials Science*, *35*, 261–270.

Ji, Y., Li, X. T., & Chen, G. Q. (2008). Interactions between a poly(3-hydroxybutyrate-*co*-3-hydroxyvalerate-*co*-3-hydroxyhexanoate) terpolyester and human keratinocytes. *Biomaterials*, *29*(28), 3807–3814.

Jung, H. Z., Benerito, R. R., Berni, R. J., & Mitcham, D. (1977). Effect of low temperatures on polymorphic structure of cotton cellulose. *Journal of Applied Polymer Science*, *21*, 1981–1988.

Klemm, D., Schumann, D., Udhardt, U., & Marsch, S. (2001). Bacterial synthesized cellulose – Artificial blood vessels for microsurgery. *Progress in Polymer Science*, *26*(9), 1561–1603.

Koning, G. J. M., & Lemstra, P. J. (1993). Crystallization phenomena in bacterial poly[(*R*)-3-hydroxybutyrate]: 2. Embrittlement and rejuvenation. *Polymer*, *34*(19), 4089–4094.

Korakot, S., Neeracha, S., Prasit, P., & Pitt, S. (2007). Bone scaffolds from electrospun fiber mats of poly(3-hydroxybutyrate), poly(3-hydroxybutyrate-*co*-3-hydroxyvalerate) and their blend. *Polymer*, *48*(5), 1419–1427.

Lee, W., Ichi, T., Ooya, T., Yamamoto, T., Katoh, M., & Yui, N. (2003). Novel poly(ethylene glycol) scaffolds crosslinked by hydrolyzable polyrotaxane for cartilage tissue engineering. *Journal of Biomedical Materials Research A*, *67*, 1087–1092.

Legeza, V. I., Galenko-Yaroshevskii, V. P., Zinov'ev, E. V., Paramonov, B. A., Kreichman, G. S., Turkovskii, I. I., et al. (2004). Effects of new wound dressings on healing of thermal burns of the skin in acute radiation disease. *Bulletin of Experimental Biology and Medicine*, *138*(3), 311–315.

Li, J., Li, X., Ni, X., Wang, X., Li, H., & Leong, K. W. (2006). Self-assembled supramolecular hydrogels formed by biodegradable PEO–PHB–PEO triblock copolymers and α-cyclodextrin for controlled drug delivery. *Biomaterials*, *27*(22), 4132–4140.

Liudmila, N. N., Jonas, P., Maria, B., Mikael, W., & Lev, N. N. (2008). Biodegradable poly-β-hydroxybutyrate scaffold seeded with Schwann cells to promote spinal cord repair. *Biomaterials*, *29*(9), 1198–1206.

Qu, X. H., Wu, Q., Liang, J., Zou, B., & Chen, G. Q. (2006). Effect of 3-hydroxyhexanoate content in poly(3-hydroxybutyrate-*co*-3-hydroxyhexanoate) on in vitro growth and differentiation of smooth muscle cells. *Biomaterials*, *27*(15), 2944–2950.

Savenkova, L., Gercberga, Z., Nikolaeva, V., Dzene, A., Bibers, I., & Kalnin, M. (2000). Mechanical properties and biodegradation characteristics of PHB-based films. *Process Biochemistry*, *35*(6), 573–579.

Scandola, M., Focarete, M. L., Gazzano, M., Matuszowic, A., Sikorska, W., Adamus, G., et al. (1997). Crystallinity-induced biodegradation of novel [(*RS*)-β-butyrolactone]-*b*-pivalolactone copolymers. *Macromolecules*, *30*, 7743–7748.

Takai, M. (1994). Bacterial cellulose composites. In R. D. Gilbert (Ed.), *Cellulose polymer blends composites*. Munich: Hanser. Chapter 13.

Tanio, T., Fukui, T., Shirakura, Y., Sanito, T., Tomita, K., kaniho, T., et al. (1982). An Extracellular poly(3-hydroxybutyrate) depolymerase from *Alcaligenes faecalis*. *European Journal of Biochemistry*, *124*, 71–77.

Tetsuya, I., Naoko, Y., & Yoshio, I. (1999). Influence of tacticity and molecular weight of poly(vinyl alcohol) on crystallization and biodegradation of poly(3-hydroxybutyric acid)/poly(vinyl alcohol) blend films. *Polymer Degradation and Stability*, *66*(2), 263–270.

Thomson, R. C., Giordano, G. G., Collier, J. H., Ishaug, S. L., Mikos, A. G., Devjani, L. M., et al. (1996). Manufacture and characterization of poly(α-hydroxy ester) thin films as temporary substrates for retinal pigment epithelium cells. *Biomaterials*, *17*(3), 321–327.

Tokoh, C., Takabe, K., Fujita, M., & Saiki, H. (1998). Cellulose synthesized by *Acetobacter xylinum* in the presence of acetyl glucomannan. *Cellulose*, *5*, 249–261.

Wang, Y. W., Wu, Q., & Chen, G. Q. (2004). Attachment, proliferation and differentiation of osteoblasts on random biopolyester poly(3-hydroxybutyrate-co-3-hydroxyhexanoate) scaffold. *Biomaterials*, *25*, 669–675.

Wojciak-Stothard, B., Curtis, A., Monaghan, W., Macdonald, K., & Wilkision, C. (1996). Guidance and activation of murine macrophages by nanometric scale topography. *Experimental Cell Research*, *223*, 426–435.

Yalpani, M., Marchessault, R. H., Moin, F. G., & Monaseterios, C. J. (1991). Syntheses of Poly(3-hydroalkanoate)(PHA) conjugated: PHA-carbohydrate and PHA-synthetic polymer. *Macromolecules*, *24*(22), 6046–6049.

Yokouchi, M., Chatani, Y., Tadokoro, H., Teranishi, K., & Tani, H. (1973). Structural studies of polyesters: 5. Molecular and crystal structures of optically active and racemic poly (β-hydroxybutyrate). *Polymer*, *14*, 267–272.

Yoshino, K., Matsuoka, R., Nogami, A. K., Araki, H., Yamanaka, S., Watanabe, K., et al. (1991). Electrical property of pyrolyzed bacterial cellulose and its interaction effect. *Synthetic Mater*, *42*, 1593–1599.

Yuki, W., Noriaki, S., Naotsugu, N., Masao, T., Kenichi, K., & Hiroshi, M. (2007). Biodegradability of poly(3-hydroxybutyrate) film grafted with vinyl acetate: Effect of grafting and saponification. *Radiation Physics and Chemistry*, *76*(6), 1075–1083.

Zahra, B. M., Ebrahim, V., Ali, H., Shojaosadati, S. A., Ramin, K., & Kianoush, K. D. (2009). Statistical media optimization for growth and PHB production from methanol by a methylotrophic bacterium. *Bioresource Technology*, *100*(8), 2436–2443.

Zhao, K., Deng, Y., Chen, J. C., & Chen, G. Q. (2003). Polyhydroxyalkanoate (PHA) scaffolds with good mechanical properties and biocompatibility. *Biomaterials*, *24*(6), 1041–1045.

Zhou, J., Peng, S. W., Wang, Y. Y., Zheng, S. B., Wang, Y., & Chen, G. Q. (2010). The use of poly(3-hydroxybutyrate-*co*-3-hydroxyhexanoate) scaffold for tarsal repair in eyelid reconstruction in the rat. *Biomaterials*, *31*(29), 7512–7518.